Marangoni effect in SiO_2 during field-directed chemical vapor deposition growth of carbon nanotubes

J. Svensson,[1] N. M. Bulgakova,[2] O. A. Nerushev,[1,2] and E. E. B. Campbell[1,*]
[1]*Department of Physics, Göteborg University, SE-41296 Göteborg, Sweden*
[2]*Institute of Thermophysics, RAS-SB, 1 Acad. Lavrentyev Ave., 630090 Novosibirsk, Russia*
(Received 30 March 2006; published 18 May 2006)

Intense local heating of SiO_2 is shown to occur during chemical vapor deposition growth of single-walled carbon nanotubes in the presence of an electric field. This gives rise to the Marangoni effect where strong convection currents are induced in the molten SiO_2 layer. Nanoscale trenches and bumps are formed in the insulating layer directly below the growing nanotube.

DOI: 10.1103/PhysRevB.73.205413 PACS number(s): 81.07.De, 68.03.Cd

I. INTRODUCTION

Surface tension modulation that causes liquid flow is known as the Marangoni effect.[1] Manifestations of this effect can be observed in many different situations. For example, the formation of wine drops from a continuous liquid film spreading over a wineglass surface is driven by the change in surface tension caused by the evaporation of alcohol.[2] Temperature gradients can also lead to the Marangoni effect and this can be an important factor, e.g., in the growth of crystals under microgravity.[3] For the first time, to the best of our knowledge, we observe the Marangoni effect in molten silicon dioxide that has been induced by strong temperature gradients formed during the growth of individual carbon nanotubes. The nanotubes supply highly localized heating of the underlying substrate leading to the formation of nanometer-scale trenches. Apart from providing a manifestation of an interesting physical effect under somewhat unexpected conditions, our work also provides considerable insight into the conditions that can arise during the field aligned growth of carbon nanotubes.

Control of the position of carbon nanotubes (CNTs) is essential for the development of applications within electronics,[4] sensors,[5] and nanoelectromechanical devices.[6] Thermal chemical vapor deposition growth techniques have the advantage of controlling the position and diameter of the individual nanotube by appropriate preparation of the catalyst particle.[7] By applying a directed gas flow[8] or by applying an electric field during growth[9,10] it has also been shown possible to control the direction of the nanotube. While exploring this method, we have observed large modifications of the underlying silicon dioxide insulator under certain conditions when the nanotubes grow from a negatively biased electrode. This is attributed to intense local heating of the underlying substrate during growth of the nanotube due to the electron field emission and associated Ohmic heating. The local field conditions at the free end of the growing nanotube can be sufficient to induce heating of the nanotube tip to temperatures on the order of 2000 K. The surface modifications can be explained in terms of convection induced by strong temperature gradients in the molten substrate immediately below the nanotube.

II. EXPERIMENT

The single-walled nanotubes are grown by thermal chemical vapor deposition (CVD) on doped Si substrates with a 400 nm thick thermally grown SiO_2 layer. Mo electrodes separated by 20 μm wide gaps are patterned using photolithography and deposited using e-gun evaporation, see Fig. 1. The catalyst used to promote the growth consists of a multilayered film of 10 nm Al_2O_3, 1 nm Fe, and 0.2 nm Mo,[11] which is patterned at the electrode tips, close to the gaps (this can be seen as the lighter region on top of the electrodes in Fig. 1). The substrate is placed on a homemade holder and contact pads are connected via Ta clamps and electrical feedthroughs to a voltage supply. The furnace, enclosing a quartz tube containing the sample, is heated in a flow of 300 SCCM H_2 and 500 SCCM Ar, where SCCM denotes cubic centimeter per minute at STP. When the temperature has reached 900 °C, Ar is switched to 500 SCCM methane which is the carbon precursor for the CNT growth. The growth proceeds for 5 min before a voltage of 20 V is applied over the electrode gaps. The applied electric field induces a dipole moment in the tubes due to their highly anisotropic polarizability[12] resulting in a force aligning the tubes with the direction of the field. The growth is performed for 20 min after which time the methane flow is switched back to Ar and the furnace is switched off.

The grown CNTs are studied by scanning electron microscopy (SEM) and tapping-mode atomic force microscopy (AFM). The majority of the nanotubes are aligned with the direction of the electric field. The electric field strength needs to be approximately 1 V/μm to align the tubes. In contrast to the results of several other groups there is no aligning effect of the gas flow.[8,13] This can be attributed to the low gas flow velocity (8.3 mm/s) in our experiments. AFM studies of the diameter distribution and Raman spectroscopy indicate that the CNTs are single walled with an average diameter of 1.6 nm and of good structural quality.

III. SURFACE MODIFICATIONS

SEM images of the electrode gaps show that a darker region surrounds the tubes growing from the negative electrode (Fig. 1). Topography studies using AFM reveal that the

 ©2006 The American Physical Society

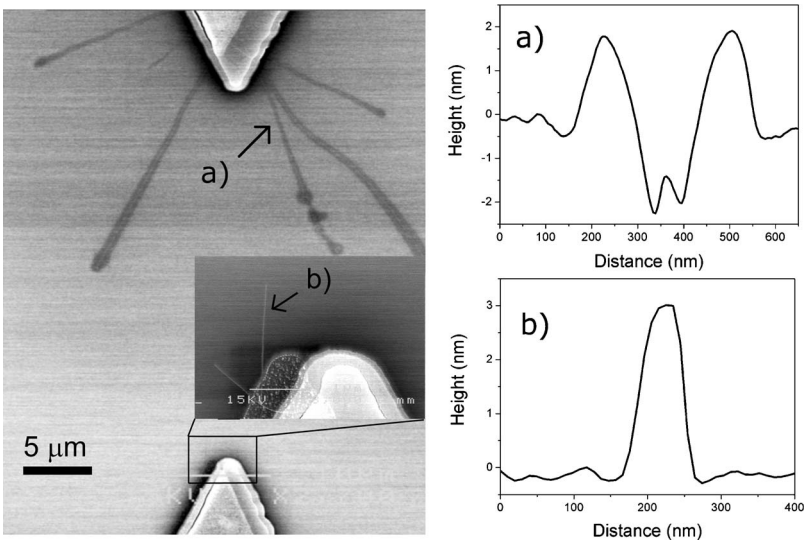

FIG. 1. Left: SEM image of a gap where the upper electrode was negatively biased and the lower electrode positively biased during growth. The dark areas surrounding the CNTs grown from the upper electrode are structural modifications of the substrate surface. Inset: higher resolution SEM picture of the nanotube shown in the AFM scan of (b). (a) AFM cross section image of a part of a nanotube grown from the upper electrode showing that the tube is embedded in a trench. (b) AFM cross section image of a nanotube grown from the lower electrode showing the nanotube lying on top of the substrate with no surface modification. Note that the lateral resolution of the AFM measurements is reduced due to tip convolution effects.

tubes are surrounded by modifications of the substrate surface. The tubes are positioned in trenches with surrounding walls that have typical widths of a few hundred nanometers, depths of a few nanometers, and are most pronounced towards the end of the nanotube [Fig. 1(a)]. No surface modifications are detected for nanotubes growing from the positive electrode [Fig. 1(b)]. Trenches of the type shown in Fig. 1 are the most common structures observed. However, it is also possible to observe modifications of the type illustrated in Fig. 2: trenches without walls and ridges with a nanotube sitting at the top of the ridge. It is also possible to observe the transition from a ridge to a trench modification along the same individual nanotube. The increasing depth of a trench along the length of a nanotube can be clearly seen in the example given in Fig. 3. The plot of depth versus length along the nanotube (measured from the negative electrode) shows a slightly greater than linear dependence and seems to saturate at a depth of 33 nm.

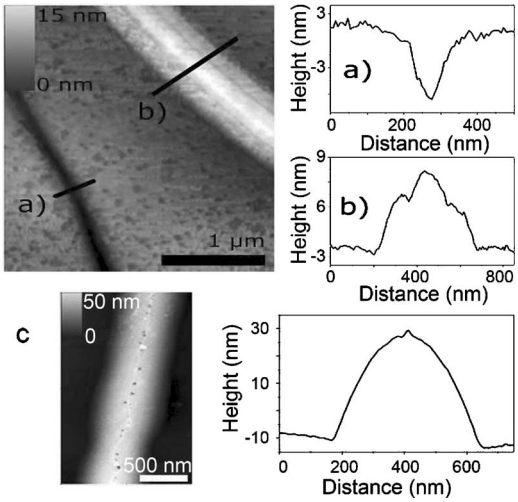

FIG. 2. AFM height profiles and cross sections of substrate modifications caused by (a) nanotubes and (b) trench ridges observed from nanotubes growing from the same electrode. The AFM lateral resolution is poor due to tip convolution effects; the nanotube shows up as a central "bump" on the AFM scan. (c) Another sample showing a much higher ridge with the nanotube clearly visible as a small bump on top of the cross section image.

The surface modifications are dependent on the growth procedure. If the electric field is applied at the beginning of the growth stage then we normally do not observe the trench structures. The trench formation is optimized if the electric field is switched on after a few minutes of growth. In this case the nanotubes start to grow close to the substrate surface. When the electric field is switched on they are then induced to follow the field lines and grow parallel and close to the substrate surface. If the electric field is applied from the beginning of the growth sequence, the nanotube is first induced to follow the field lines perpendicular to the substrate surface and will, on average, be further above the substrate during the growth.

It is possible to remove the nanotubes situated at the bottom of trenches by heating to 450 °C in air for 1 h. AFM studies have revealed that the material surrounding the tubes is not affected by this treatment, indicating that it is not a carbon deposit but it is some modification of the SiO_2 surface. The SEM images also indicate that the material in the trenches is not conductive since it appears dark.

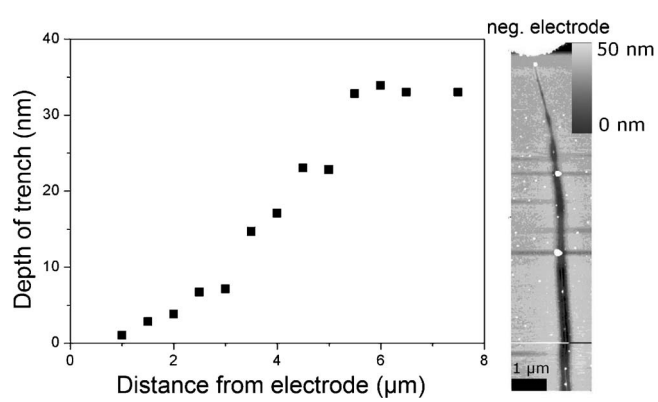

FIG. 3. Right: AFM height profile showing a long nanotube-induced trench. The nanotube can still be seen at the bottom of the trench which increases in width and depth as the nanotube extends away from the electrode. Left: Trench depth versus distance from the electrode.

IV. DISCUSSION

Since the surface modifications are only observed if the nanotube is attached to the negative electrode during growth we can rule out effects due solely to the magnitude of the field (e.g., discharges). We clearly require a supply of electrons in the presence of a strong field to generate the observed surface modifications. This implies that electron field emission could be responsible for the observations. Modeling of the local electric field around the tip of the growing nanotube using finite element simulations yields electric fields on the order of some V/nm. This is very similar to the magnitude of local fields that are needed for efficient electron field emission from individual nanotubes.[14,15] It has been shown that nanotubes that undergo strong electron field emission can be heated to temperatures on the order of 2000 K by Ohmic heating.[14–16] From the fields and geometries existing in our experiments we can expect that field emission currents on the order of μA and temperatures on the order of 2000 K are being reached. For a given field emission current, the temperature at the tip of the nanotube is higher for longer nanotubes (approximately proportional to length).[17] If the substrate modifications are predominantly an effect of the very high temperature, then this would be expected to be more pronounced for shorter distances between the nanotube and the underlying substrate, the conditions prevailing when the aligning electric field is switched on after growth has begun. We, therefore, attribute the large surface modifications to a strong local heating of the substrate immediately below the nanotube due to a combination of radiative and electron impact heating. Although the electron kinetic energy is rather low there is a high current density and this can also be expected to contribute to the local heating of the underlying substrate. However, the length dependence (Fig. 3) and the dependence on the distance of the growing nanotube from the substrate would seem to argue in favor of a temperature related effect.

It has recently been shown that temperatures at the tip of carbon nanotubes undergoing strong electron field emission can easily reach values of 2000 K. This is in agreement with experimental observations of the energy distributions of the emitted electrons from individual nanotubes[14] and of blackbody radiation measurements.[15] Such an elevated temperature is also needed to explain the shape of the field emission dependence on applied voltage for individual nanotubes studied in a combined scanning tunnelling microscopy–transmission electron microscopy (STM-TEM) setup.[16]

We will now consider whether the radiative energy emitted from the growing nanotube can be sufficient to melt the underlying SiO_2. We can approximate the melted region in the fused silica by a half-cylinder with a radius $R=200$ nm. To heat the half-cylinder volume from the nanotube growth temperature (1173 K) to the melting (softening) temperature of fused silica (2006 K),[18] the following heat energy is required:

$$Q_m = \frac{\pi R^2}{2} L c_p \Delta T. \tag{1}$$

Here L is the nanotube length (taken to be 10 μm) and c_p is the specific heat of fused silica [$\sim 2.2\times 10^6$ J/(m^3 K)]. This gives an estimate of the required melting energy to be 10^{-9} J.

The Joule heat released due to the current flow through the nanotube can be written as

$$Q_J = I^2 R t = I^2 \rho_n L t, \tag{2}$$

where ρ_n is the nanotube resistance (taken to be 10 kΩ/μm, based on Ref. 19 but taking the elevated temperature into consideration) and t is the growth time, or time during which the potential is applied (1200 s). Taking a current density of 10^8 A/cm^2, appropriate for the maximum current density for CVD-grown individual SWNT,[19] corresponding to a current through the nanotube tip of 2 μA, the Joule heating during the growth period can be estimated to be 5×10^{-4} J, much higher than the amount of energy needed to melt the underlying substrate. Not all of this energy is available for melting, however. If we assume that the main source of the melting energy is due to blackbody radiation from the nanotube then we should consider the Stefan-Boltzmann law and write the expression for the radiative energy loss

$$Q_{rad} = 2\pi r \varepsilon \sigma (T^4 - T_0^4) L t, \tag{3}$$

where r is the radius of the nanotube (8 Å), ε is the nanotube emissivity, σ is the Stefan-Boltzmann constant, and T_0 is the ambient temperature (1173 K). Assuming true black bodylike behavior ($\varepsilon=1$) this would yield an energy of 5×10^{-5} J. Even considering a lower limit for the emissivity of 10^{-3}, based on that measured for fullerenes,[20] and considering the spatial distribution of the radiation we still have an estimate of the radiated energy at the substrate that is approximately one order of magnitude higher than required for melting.

Since the nanotube is anchored at one end to the electrode, which is therefore at the ambient temperature, there will be a temperature gradient along the nanotube[16] leading to higher melting effects as the nanotube increases in length (due to both the higher temperature reached at the tip of the nanotube and the correspondingly higher electron emission current at the elevated temperature). This can explain, e.g., the trench depth dependence on length shown in Fig. 3 and the increasing width of the black traces in the SEM picture shown in Fig. 1. The thermal conductivity of the fused silica is very small so that the energy absorbed from the nanotube radiation can be expected to be confined in the near-nanotube region for a relatively long time.

The strong local heating and high temperature gradients in the substrate below the nanotube will lead to surface tension gradients in the liquid that will induce convective motion known as the Marangoni effect.[1] At the free surface, the Marangoni effect occurs due to the shear stress which is equal to the gradient of the temperature dependent surface tension s along the melt surface. The velocity of the liquid on the surface can be estimated as

$$\eta \frac{\partial u_x}{\partial n} = \frac{\partial s}{\partial x} = \frac{\partial s}{\partial T}\frac{\partial T}{\partial x}, \tag{4}$$

where η is the dynamic viscosity, n is the coordinate normal to the liquid surface, and x is the coordinate tangential to the surface. Marangoni convection can result from a geometrical

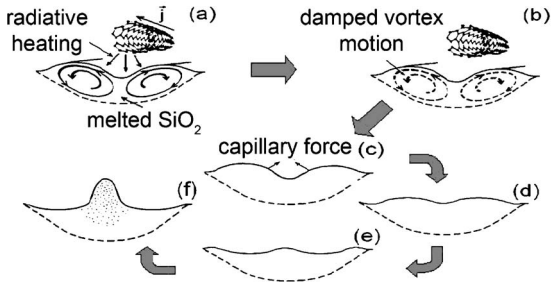

FIG. 4. Schematic diagram of the Marangoni effect.

asymmetry of local energy sources and it is known as an effect inherent to laser welding.[21,22] The Marangoni effect frequently causes surface deformation where the form of the deformation depends on the sign of ds/dT.[23] For most liquids including silica, the surface tension decreases with increasing temperature so the Marangoni convection results in vortex motion and liquid movement towards the region of decreasing temperature. This is illustrated in Fig. 4. When the nanotube growth has been completed the liquid trench on the silica surface below the nanotube will start to cool down. This results in a decrease of the temperature and surface tension gradients and the convective motion originating from the Marangoni effect will be damped [Fig. 4(b)]. The hydrodynamic motion will then evolve in the following way. Due to the surface tension, capillary waves will be generated [Fig. 4(c)]. The capillary waves will exist in the liquefied region until the fused silica congeals during cooling due to thermal conductivity. The surface topology will then change in the sequence shown in Figs. 4(d)–4(f). The amplitude of the surface wave will first decrease [Fig. 4(d)], transforming to its mirror image [Fig. 4(e)] by passing a phase where there is a practically smooth surface. This sequence of events will result in a splashing of material along the liquid trench axis [Fig. 4(f)]. After this, the sequence will be repeated in inverse order [Figs. 4(e)→ 4(d)→4(c)] Thus, any surface topology can be frozen due to the described hydrodynamical motion and the gradual cooling: a trench with walls [Fig. 4(c)], a bump [Fig. 4(f)], or an almost flat surface (the intermediate phase between the bump and the trench). The final structure will strongly depend on the initial temperature of the liquid and the size of the liquid zone. We have noted that the bumps are rather unstable and are easily removed when attempting to bond to electrodes deposited on top of them, leaving behind a trench. This may be due to the porosity of the material. Porosity will arise in molten flowing matter either when the momentum is small and, thus, not able to completely destroy the continuity of matter or when the velocity gradients are low.[24] After solidification, such material will form a porous fragile structure. It is possible that the state of the slowly flowing fused silica can reach the limit of tensile strength resulting in a high porosity after solidification [Fig. 4(f)]. An alternative mechanism for bump formation could be the occurrence of high temperature gradients leading to thermal stress in the locally heated matter which, remaining solid, loses strength.[25] This would be expected to lead to the formation of a trench without walls after a bump destruction, as we do indeed observe in some cases [Fig. 2(a)]. At present we cannot rule out this mechanism as an additional contributing factor to the Marangoni effect in the limit of fused silica melting. Alternatively, the simple trench structures that are occasionally observed may be due to vaporization of the fused silica.

We have observed similar effects when applying a negative bias to nanotubes at elevated temperatures (1000 °C) after growth, under conditions where significant electron field emission is expected. It may thus be possible to develop a controlled nanoscale heating using patterned carbon nanotubes as a means of nanometric modification of surfaces.

V. CONCLUSION

In conclusion, we have shown the occurrence of the Marangoni effect in silica substrates that have been locally heated by single-walled nanotubes grown in the presence of an electric field ($\geqslant 1$ V/μm). The effect can only be observed when the nanotube grows from an electrode that has been negatively biased. It has never been observed from the positively biased electrode. The local fields at the tip of the growing nanotube are strong enough to induce significant electron field emission and we attribute the observed effects to a strong local heating of the underlying substrate via thermal radiation from the nanotube (with a possible contribution from electron bombardment of the substrate). The high temperatures ($\sim$2000 K) needed to induce local melting in the underlying substrate can be produced in the nanotube by Ohmic heating due to the high field emission currents (on the order of a few μA). Sublimation of fused silica may play a role in the trench formation but a simple estimate shows that it is difficult to explain the magnitude of the structures with this mechanism, and, more importantly, it cannot explain the elevated regions along the edges of the trenches or the bump formation that is occasionally observed. All these structures can be easily explained within the Marangoni picture. Surface diffusion, which can be an effective mass transport mechanism on the nanometric scale and would, in principle, require lower temperatures, can also be ruled out. The driving force for surface diffusion is the minimization of the surface free energy. This typically leads to a smoothing of surfaces rather than a roughening that is observed here. Also, it would be difficult to explain the three kinds of observed structures if the main effect was surface diffusion (leading to both trench formation, with and without "walls" and ridge formation) whereas these structures emerge naturally from a consideration of the Marangoni effect.

ACKNOWLEDGMENTS

This work was supported financially by Stiftelsen för Strategisk Forskning (SSF) within the CARAMEL consortium and by Vetenskapsrådet. The authors thank S. Dittmer for help with preparing the substrates and Y. P. Meshcheryakov for useful discussions.

*Corresponding author. Electronic address:
Eleanor.Campbell@physics.gu.se

[1] L. E. Scriven and C. V. Sternling, Nature (London) **187**, 186 (1960).
[2] J. Thomson, Philos. Mag. **10**, 330 (1855).
[3] K. Kinoshita and T. Yamada, J. Cryst. Growth **96**, 953 (1989).
[4] P. L. McEuen, M. S. Fuhrer, and H. Park, IEEE Trans. Nanotechnol. **1**, 1 (2002).
[5] J. Kong, N. R. Franklin, C. Zhou, M. G. Chapline, C. Peng, K. Cho, and H. Dai, Science **287**, 622 (2000).
[6] T. Rueckes, K. Kim, E. Joselevich, G. Y. Tseng, C.-L. Cheung, and C. M. Lieber, Science **289**, 5476 (2000).
[7] M. Ishida, H. Hongo, F. Nihey, and Y. Ochiai, Jpn. J. Appl. Phys., Part 2 **43**, L1356 (2004).
[8] S. Huang, M. Woodson, R. E. Smalley, and J. Liu, Nano Lett. **4**, 6 (2004).
[9] E. Joselevich and C. M. Lieber, Nano Lett. **2**, 10 (2002).
[10] A. Ural, Y. Li, and H. Dai, Appl. Phys. Lett. **81**, 18 (2002).
[11] L. Delzeit, B. Chen, A. Cassell, R. Stevens, C. Nguyen, and M. Meyyappan, Chem. Phys. Lett. **348**, 368 (2001).
[12] L. X. Benedict, S. G. Louie, and M. L. Cohen, Phys. Rev. B **52**, 8541 (1995).
[13] S. Li, Z. Yu, C. Rutherglen, and P. J. Burke, Nano Lett. **4**, 10 (2004).
[14] S. T. Purcell, P. Vincent, C. Journet, and V. T. Binh, Phys. Rev. Lett. **88**, 105502 (2002).
[15] M. Sveningsson, M. Jonsson, O. A. Nerushev, F. Rohmund, and E. E. B. Campbell, Appl. Phys. Lett. **81**, 1095 (2002).
[16] M. Sveningsson, K. Hansen, K. Svensson, E. Olsson, and E. E. B. Campbell, Phys. Rev. B **72**, 085429 (2005).
[17] M. Sveningsson, R. Morjan, O. Nerushev, K. Svensson, E. Olsson, and E. E. B. Campbell, in *Fullerenes and Nanotubes: The Building Blocks of Next Generation Nanodevices*, edited by D. M. Guldi, P. V. Kamat, and F. D'Souza (Electrochemical Soc., New York, 2003), pp. 340–345.
[18] J. Siegel, K. Ettrich, E. Welsch, and E. Matthias, Appl. Phys. A **64**, 213 (1997).
[19] J. Kong, C. Zhou, A. Morpurgo, H. T. Soh, C. F. Quate, C. Marcus, and H. Dai, Appl. Phys. A **69**, 305 (1999).
[20] M. Hedén, K. Hansen, F. Jonsson, E. Rönnow, A. Gromov, A. Taninaka, H. Shinohara, and E. E. B. Campbell, J. Chem. Phys. **123**, 044310 (2005).
[21] T. Fuhrich, P. Berger, and H. Hügel, J. Laser Appl. **13**, 178 (2001).
[22] X. He, T. DebRoy, and P. W. Fuerschbach, J. Appl. Phys. **94**, 6949 (2003).
[23] D. Bäuerle, *Laser Processing and Chemistry*, 3rd ed. (Springer-Verlag, New York, 2000).
[24] F. A. Baum, L. P. Orlenko, K. P. Stanyukovich, R. P. Chelyshev, and B. I. Shekhter, *Physics of Explosion* (Moscow, Nauka, 1975) (in Russian).
[25] Yu. P. Meshcheryakov and N. M. Bulgakova, Appl. Phys. A **82**, 363 (2006).